



INTERNATIONAL ATOMIC ENERGY AGENCY  
UNITED NATIONS EDUCATIONAL, SCIENTIFIC AND CULTURAL ORGANIZATION  
**INTERNATIONAL CENTRE FOR THEORETICAL PHYSICS**  
I.C.T.P., P.O. BOX 586, 34100 TRIESTE, ITALY, CABLE: CENTRATOM TRIESTE



SMR.755/13

**Workshop on Fluid Mechanics**

**(7 - 25 March 1994)**

**Compositional Convection:  
The stability of double-diffusive  
vertically oriented interfaces**

I.A. Eltayeb  
Department of Mathematics and Computing  
College of Science  
Sultan Qaboos University  
Muscat  
Sultanate of Oman

**COMPOSITIONAL CONVECTION :**

**THE STABILITY OF DOUBLE-DIFFUSIVE VERTICALLY  
ORIENTED INTERFACES**

By

Ibrahim A.Eltayeb

Department of Mathematics and Computing , College of  
Science,Sultan Qaboos University , Muscat , Sultanate of Oman

Lecture delivered to the " Workshop on Fluid Mechanics " held at the International Centre for Theoretical Physics , Trieste , Italy , During the period 7 - 25 March, 1994

## 1. INTRODUCTION

The magnetic fields of some celestial bodies like the Earth and Sun have long been of interest to physicists because they seem to have maintained themselves for a long time. It is now known that the magnetic field of the Earth has maintained its strength for a time much longer than its free decay time of about  $4.5 \times 10^3$ . That result was one of the reasons why the Earth must have a fluid core. The presence of a fluid core of an electrically conducting fluid permits the interaction of the fluid flow and the magnetic lines of force to produce an e.m.f. which helps the magnetic field to regenerate itself (Moffatt, 1978). The subject of the study of the process of regeneration of a magnetic field is known as dynamo theory (because of the similarity with the simple electrical dynamo).

The dynamo problem is generally composed of the equations of motion of an electrically conducting fluid together with those of magnetic induction, energy and state. This is a fluid dynamics problem. The complexity of the problem is due to its nonlinearity and a full solution is extremely difficult to find. Consequently, a host of simpler but relevant problems have posed themselves as essential for the understanding of the dynamo process. These include many of the problems dealing with motions in rotating and/or electrically conducting problems.

Four decades ago, it was believed that the main source of energy to power the geo-dynamo was thermal, with the heat being produced by radio-active materials (e.g.,  $K^{40}$ ) in the Earth's Outer Fluid Core (OFC) See Fig.1. This led to many studies on the thermal stability of rotating and / or magnetic fluids (see, e.g., Chandrasekhar, 1961; Eltayeb, 1972, 1975, 1984, 1992; Roberts and Stewartson 1974, Eltayeb & Kumar, 1977; Fearn 1979).

Recently it has been realised that the heat supply due to radio-active materials in the Earth's core is insufficient to drive a dynamo with a large toroidal field like that expected to be in the Earth's OFC, particularly in view of the fact that a thermal engine is not a very efficient one. The gravitationally powered dynamo was then proposed. The reader is referred to the series of papers by Loper and collaborators (Loper & Roberts, 1983, Roberts and Loper 1983, Loper 1983, 1984).

The OFC of the Earth is assumed to be composed of an alloy of iron and one or more lighter elements (e.g., sulphur, oxygen). The distribution of temperature and pressure in the OFC is such that freezing of the iron component takes place near the Inner Core Boundary (ICB). This leads to the formation of a mushy zone on the surface of the Inner Core containing a mixture of the solid heavy element (iron) and light fluid element. The light fluid escapes in thin helical fluid filaments (called compositional plumes) to the upper reaches of the OFC thereby producing convective motions which interact with the magnetic field to produce a dynamo mechanism. The studies by Loper and collaborators have shown that such a mechanism is capable of sustaining a large toroidal field in the Earth's Core.

The solution of the gravitationally powered dynamo is not easier than the thermal dynamo problem. It is then necessary to investigate simpler problems which deal with some aspect of the gravitationally powered dynamo in order to gain some insight into the physical mechanism of this dynamo process.

Simple laboratory experiments on the freezing of fluid alloys can be made. A popular one is the ammonium chloride solution. Here a 30% by weight ammonium chloride solution in water is raised to a temperature of about 50 C. The solution is contained in a beaker and the beaker is placed on a cold surface. After a while the ammonium chloride will start to crystallize and a mushy zone forms at the bottom of the beaker. When the thickness of the mushy zone increases to a certain value, the fresh water in the mushy zone begins to rise in thin helical plumes (see Fig. 2). The flow associated with these compositional plumes is not known and the stability of such flows is of interest to the dynamo problem.

The basic problem associated with the plumes is the dynamic influence of the interface between two fluids of different composition: the fluid within the plumes is solely of the light element of the alloy while the surrounding fluid is the (mixed) alloy fluid.

The flow associated with these plumes has been studied by Eltayeb and Loper (1991) for the classical case in which both rotational and magnetic effects are absent. Addition of vertical

rotation leads to the same basic flow but the presence of the magnetic field modifies the flow considerably.

In order to provide the best possible way to understand the physical mechanisms involved it was necessary to consider simple models which compare with other problems of a similar mathematical nature. The problem of the heated vertical wall studied by Gill and Davey (1969), Dudis and Davis (1971) provided a convenient problem to compare with. We therefore consider first the problem in which a single interface separates two semi-infinite fluids of different composition. This case is referred to as the *single line interface*. Next we consider the case of two parallel interfaces. This model is referred to as the *cartesian plume*. This model has the advantage of adding the complexity of a second interface but is simple enough to avoid the effects of curvature. The problem of the helical plume was also considered by Eltayeb and Loper (1991) but is not included here.

Here the basic flow is identified for both the single line interface and the cartesian plume in the presence of rotation and magnetic field. The stability of the single line plume only is considered. The influence of rotation on the compositional mode of instability is examined. The stability of the non-rotating cartesian plume can be found in Eltayeb and Loper (1994).

## 2. FORMULATION

Consider a fluid whose density depends both on temperature and material composition. Suppose that the Boussinesq approximation is applicable so that

$$\rho/\rho_0 = 1 - \alpha(T - T_0) - \beta(C - C_0) \quad (2.1)$$

where  $\rho$  is the density,  $\alpha$  is the coefficient of volume expansion,  $\beta$  is the coefficient of compositional expansion,  $T$  is the temperature,  $C$  is the concentration of light material and  $o$  denotes a

constant reference value. The fluid is flowing with velocity  $\mathbf{u}$  in a frame of reference which rotates vertically with angular speed  $\Omega$  in the presence of a magnetic field  $\mathbf{B}$ . The equations are those of linear momentum, mass conservation, energy, induction and buoyant material. They are, respectively,

$$\begin{aligned} \partial \mathbf{u} / \partial t + \mathbf{u} \cdot \nabla \mathbf{u} + 2\Omega \hat{\mathbf{z}} \times \mathbf{u} = \\ -\nabla p + \nu \nabla^2 \mathbf{u} + (\mu \rho_0)^{-1} \nabla \times \mathbf{B} \times \mathbf{B} + \rho g / \rho_0 \end{aligned} \quad (2.2)$$

$$\nabla \cdot \mathbf{u} = 0 \quad (2.3)$$

$$\partial T / \partial t + \mathbf{u} \cdot \nabla T = \kappa \nabla^2 T \quad (2.4)$$

$$\partial \mathbf{B} / \partial t = \nabla \times (\mathbf{u} \times \mathbf{B}) + \nabla^2 \mathbf{B}, \quad \nabla \cdot \mathbf{B} = 0 \quad (2.5)$$

$$\partial C / \partial t + \mathbf{u} \cdot \nabla C = 0 \quad (2.6)$$

Here  $p$  is the pressure,  $\mu$  the magnetic permeability,  $\nu$  the kinematic viscosity,  $\kappa$  the thermal diffusivity,  $\eta$  the magnetic diffusivity,  $\mathbf{g}$  the gravitational acceleration and we shall always adopt the notation that  $\hat{\mathbf{x}}$  is a unit vector along the x-axis. The z-axis is chosen to be vertically upwards. The Boussinesq approximation, in which the density variations are neglected unless they occur in the gravity term in the equation of motion, has been adopted.

We now express the equations (2.2) - (2.6) into dimensionless form. We take  $\tilde{C}$  and  $\tilde{B}$  as typical amplitudes of the material concentration and magnetic field and  $\gamma$  as the vertical temperature gradient. Define a length scale

$$L = (\kappa \nu / \alpha \gamma g)^{1/4} \quad (2.7)$$

and an associated time scale

$$\tau = (\kappa / \alpha \gamma \nu g)^{1/2} \quad (2.8)$$

$L$  is the usual salt-finger length scale and  $\tau$  is the associated viscous time scale. We shall use these two as units of length and time respectively. Also let  $u (= \beta \bar{C} (g \kappa / \alpha \gamma \nu)^{1/2})$ ,  $\beta \bar{C} / \alpha$ ,  $\rho_0 \beta \bar{C} (g^3 \nu \kappa / \alpha \gamma)^{1/4}$  be the units of velocity, temperature and pressure difference, respectively. The dimensionless equations can now be written as

$$\begin{aligned} \partial u / \partial t + R u \nabla u + T a^{1/2} \hat{z} \times u = \\ -\nabla \Pi + \nabla^2 u + Q (\sigma_m R)^{-1} (B \cdot \nabla) B + (C - C_0 + T - T_0) \hat{z} \end{aligned} \quad (2.9)$$

$$\sigma (\partial / \partial t + R u \cdot \nabla) T = \nabla^2 T \quad (2.10)$$

$$\sigma_m \partial B / \partial t = \sigma_m R \nabla \times (u \times B) + \nabla^2 B \quad (2.11)$$

$$(\partial / \partial t + R u \cdot \nabla) C = 0 \quad (2.12)$$

These equations show that the problem posed here is governed by four dimensionless parameters: the Prandtl number  $\sigma$ , the magnetic Prandtl number  $\sigma_m$ , the Reynolds number  $R$  and the Chandrasekhar number  $Q$  (which is the square of the Hartmann number  $M$ ). They are defined by

$$\begin{aligned} \sigma = \frac{\nu}{\kappa}, \sigma_m = \frac{\nu}{\eta}, R = \beta \bar{C} (g \kappa^3 / \alpha^3 \gamma^3 \nu^5)^{1/4} = \frac{UL}{\nu}, \\ Q = \frac{B_0^2}{\mu \nu \eta \rho_0} \left( \frac{\nu \kappa}{\alpha \gamma g} \right)^{1/2} \end{aligned} \quad (2.13)$$

In (2.9)  $\Pi$  is the total pressure defined by

$$\Pi = p - (z - z_0) / \beta \bar{C} + (z - z_0)^2 / 2 \sigma R + Q B^2 / 2 \sigma_m R \quad (2.14)$$

A solution of these equations is sought in the form

$$\begin{aligned} u &= \bar{w}(x) \hat{z} + \varepsilon u^* \\ T &= T_0 + (z - z_0) / \sigma R + \bar{T}(x) + \varepsilon T^* \\ C &= C_0 + \bar{C}(x) + \varepsilon C^* \\ \Pi &= p_0 + \bar{p}(x) + \varepsilon p^* \\ B &= \bar{x} + \sigma R \bar{b}(x) + \varepsilon \sigma R b^* \end{aligned} \quad (2.15)$$

The quantities with an 'overbar' depend on the horizontal coordinate  $x$  only. They denote the basic solution while the quantities with the superscript '\*' denote the perturbations of small amplitude  $\varepsilon$ , which depends on the vertical coordinate  $z$ , on the second horizontal coordinate  $y$  and on time. We shall first find the exact solutions of the basic variables. The equations governing the basic variables are obtained by setting  $\varepsilon = 0$  in (2.15) and using equations (2.9) - (2.12).

#### The basic equations and their solution

Since the basic state variables depend on  $x$  only we have

$$\begin{aligned} 0 &= -\nabla \bar{p} + (D^2 \bar{w} + Q D \bar{b} + \bar{T} + \bar{C}) \hat{z}, \\ 0 &= \bar{w} - D^2 \bar{T}, \quad 0 = D \bar{w} + D^2 \bar{b} \end{aligned} \quad (2.16)$$

where

$$D \equiv d/dx \quad (2.17)$$

~~we consider~~ We shall consider two separate cases below. The first is the *single line interface*, in which

$$\bar{C} = -\frac{1}{2} \operatorname{sgn}(x) \quad (2.18)$$

so that the fluid is light for  $x < 0$  and heavy for  $x > 0$ . The interface of discontinuity for material concentration is  $x = 0$ . The boundary conditions then are

- (1)  $\bar{w}, \bar{T}, \bar{b}$  are finite as  $x \rightarrow \pm \infty$
- (2)  $\bar{w}, \bar{T}, \bar{b}$  are regular at  $x = 0$
- (3)  $\bar{w}, \bar{T}, \bar{b}, D\bar{w}, D\bar{T}$  are continuous at  $x = 0$  (2.19)

The solution of (2.16)-(2.19) can readily be written down as

$$\bar{T} = \pm \frac{1}{2} \{ 1 + \chi | \alpha_2^2 \exp(\mp \alpha_1 x) - \alpha_1^2 \exp(\mp \alpha_2 x) | \} \quad (2.20)$$

$$\bar{w} = \pm \frac{1}{2} \chi | \exp(\mp \alpha_1 x) - \exp(\mp \alpha_2 x) | \quad (2.21)$$

$$\bar{b} = \frac{1}{2} \chi | \alpha_2 \exp(\mp \alpha_1 x) - \alpha_1 \exp(\mp \alpha_2 x) | \quad (2.22)$$

in which the upper ( lower ) sign refers to  $x > ( < ) 0$ . We note that the basic temperature and velocity are odd functions of  $x$  while the basic magnetic field is even. Here we have defined

$$\alpha_{1,2} = \left\{ Q/2 \pm \sqrt{Q^2/4 - 1} \right\}^{1/2}, \quad \chi^{-1} = \alpha_1^2 - \alpha_2^2, \quad \operatorname{Re}(\alpha_{1,2}) > 0 \quad (2.23)$$

The solutions (2.20)-(2.23) depend strongly on the magnetic field strength as measured by the Chandrasekhar number  $Q$ . The profiles of these functions are illustrated in Fig. 3. When the magnetic field is absent ( i.e.,  $Q = 0$  ), the solutions are oscillatory but as  $Q$  increases from zero, the oscillations tend to be suppressed. When  $Q$  exceeds 2 the oscillations disappear completely.

~~The solution (2.20)-(2.22) is associated with material, heat and buoyancy fluxes  $F_m, F_H$  and  $F_B$ , respectively, defined by~~

The solution (2.20)-(2.22) is associated with material, heat and buoyancy fluxes  $F_m, F_H$  and  $F_B$ , respectively, defined by

$$F_m = \frac{1}{\ell} \int w C dA, \quad F_H = \frac{1}{\ell} \int w T dA, \quad F_B = \alpha F_H + \beta F_m \quad (2.24)$$

where the integrals are taken over a specified horizontal area and  $\ell$  is a measure of the horizontal length scale of the interface. We use

$$\beta^2 \bar{C}^2 (g \kappa^3 / \nu \alpha^3 \gamma^3)^{1/4}, \quad \beta \bar{C}^2 (g \alpha \kappa^3 / \nu \gamma^3)^{1/4}, \quad \beta^2 \bar{C}^2 (g \alpha \kappa^3 / \nu \gamma^3)^{1/4} \quad \text{as units of}$$

$F_H, F_m, F_B$  to find that the dimensionless fluxes are

$$F_H = \int_{-\infty}^{\infty} \bar{w} \bar{T} dx, \quad F_m = \int_{-\infty}^{\infty} \bar{w} \bar{C} dx, \quad F_B = F_H + F_m \quad (2.25)$$

These integrals can be calculated from (2.20) - (2.22) to find that

$$F_m = \frac{1/2}{(\alpha_1 + \alpha_2)}, \quad F_H = \frac{-(Q+3)/4}{(\alpha_1 + \alpha_2)(Q+2)}, \quad F_B = \frac{(Q+1)/4}{(\alpha_1 + \alpha_2)(Q+2)} \quad (2.26)$$

The fluxes are also strongly dependent on the strength of the magnetic field (see Fig. 4)

The second case we consider is the *cartesian plume*. Here we assume the top-hat profile for the basic concentration:

$$\bar{C} = \begin{cases} 1 & \text{for } |x| < x_0 \\ 0 & \text{for } |x| > x_0 \end{cases} \quad (2.27)$$

Here we solve (2.16) subject to the boundary conditions (2.19) provided we apply (2) and (3) at  $x_0$  and  $-x_0$ . The solutions can be written as

$$\bar{T} = \begin{cases} \chi [\alpha_2^2 S_1 \exp(-\alpha_1|x|) - \alpha_1^2 S_2 \exp(-\alpha_2|x|)] ; |x| > x_0 \\ \chi [-\alpha_2^2 E_1 \cosh(\alpha_1 x) + \alpha_1^2 E_2 \cosh(\alpha_2 x)] - 1 ; |x| < x_0 \end{cases} \quad (2.28)$$

$$\bar{w} = \begin{cases} \chi [S_1 \exp(-\alpha_1|x|) - S_2 \exp(-\alpha_2|x|)] ; |x| > x_0 \\ \chi [-E_1 \cosh(\alpha_1 x) + E_2 \cosh(\alpha_2 x)] ; |x| < x_0 \end{cases} \quad (2.29)$$

$$\bar{b} = \begin{cases} \chi [\alpha_2 S_1 \exp(-\alpha_1|x|) - \alpha_1 S_2 \exp(-\alpha_2|x|)] ; |x| > x_0 \\ \chi [\alpha_2 E_1 \sinh(\alpha_1 x) - \alpha_1 E_2 \sinh(\alpha_2 x)] ; |x| < x_0 \end{cases} \quad (2.30)$$

in which

$$\begin{aligned} S_1 &= \sinh(\alpha_1 x_0), & S_2 &= \sinh(\alpha_2 x_0), \\ E_1 &= \exp(-\alpha_1 x_0), & E_2 &= \exp(-\alpha_2 x_0) \end{aligned} \quad (2.31)$$

The behaviour of this solution is illustrated in Fig. 5. We again see that the solution is oscillatory for small  $Q$ . As  $Q$  increases beyond 2 the oscillations disappear. It is also noticeable that the amplitude of the solutions decreases with  $Q$  so that the magnetic field tends to reduce the vigour of the motions. We should mention here that the apparent singularity at  $Q=2$  is not a real one and a detailed study of the solutions near  $Q=2$  reveals that the solutions are well-behaved there.

The ( dimensionless ) fluxes of material, heat and buoyancy can be found by integrating the functions (2.28)- (2.31). It is informative to write the expressions for the three cases of  $Q$  greater, equal or less than 2, separate.

For  $Q < 2$

$$\begin{aligned} F_H &= F_B - F_m, & \Lambda &= \sqrt{1-Q^2/4} \\ F_m &= (2\Lambda)^{-1} \left\{ b - \exp(-2ax_0) [a \sin(2bx_0) + b \cos(2bx_0)] \right\} \end{aligned}$$

$$\begin{aligned} F_B &= \frac{1}{4} F_m + (4\Lambda^3)^{-1} \left\{ x_0 \Lambda^2 \exp(-2ax_0) \sin(2bx_0) \right. \\ &\quad \left. + \frac{1}{2} Q b^3 [1 - \exp(-2ax_0) \cos(2bx_0)] \right. \\ &\quad \left. + \frac{Q}{2} [a^3 \sin(2bx_0) - x_0 \Lambda \cos(2bx_0)] \exp(-2ax_0) \right\} \end{aligned} \quad (2.32)$$

For  $Q = 2$ :

$$\begin{aligned} F_m &= \frac{1}{4} [1 - (1+2x_0) \exp(-2x_0)], \\ F_B &= \frac{3}{32} [1 - (1+2x_0 - \frac{8}{3}x_0^2 - \frac{8}{9}x_0^3) \exp(-2x_0)] \end{aligned} \quad (2.33)$$

For  $Q > 2$ :

$$\begin{aligned} F_m &= (4\chi)^{-1} [\alpha_1 - \alpha_2 + \alpha_2 \exp(-2\alpha_1 x_0) - \alpha_1 \exp(-2\alpha_2 x_0)], \\ F_B &= \frac{1}{4} F_m + (8\chi^2)^{-1} \left\{ \frac{Q(Q/2-1)}{2(\alpha_1+\alpha_2)} + \right. \\ &\quad \left. x_0 \chi [\exp(-2\alpha_2 x_0) - \exp(-2\alpha_1 x_0)] + \right. \\ &\quad \left. \frac{Q}{8\chi} (\alpha_1 - \alpha_2) [(1-\alpha_2^2) \exp(-2\alpha_2 x_0) + (1-\alpha_1^2) \exp(-2\alpha_1 x_0)] + \right. \\ &\quad \left. \frac{Q(\alpha_1+\alpha_2)}{4\chi} [(-1+x_0(\alpha_1-\alpha_2)) \exp(-2\alpha_2 x_0) + \right. \\ &\quad \left. (1+x_0(\alpha_1-\alpha_2)) \exp(-2\alpha_1 x_0)] \right\} \end{aligned} \quad (2.34)$$

The dependence of the fluxes on  $Q$  and  $x_0$  are illustrated in Fig.6.

### 3. The stability Analysis

In this section we examine the stability of the basic state solution to disturbances of a single interface separating two fluids of different material composition (see Fig.7). The perturbation equations can be obtained by substituting (2.15) into (2.9) - (2.12) and subtracting (2.16) :

$$\begin{aligned} \partial u^*/\partial t + R[\bar{w}\partial u^*/\partial z + (u^*\hat{x})\bar{w}'\hat{z} + Ta^{1/2}\hat{z} \times u^*] = \\ -\nabla p^* + \nabla^2 u^* + QDb^* \\ + Q\sigma_m R[\bar{b}\partial b^*/\partial z + (b^*\hat{x})\bar{b}'\hat{z}] + (C^* + T^*)\hat{z} \end{aligned} \quad (3.1)$$

$$\sigma\partial T^*/\partial t + \sigma R[\bar{w}\partial T^*/\partial z + (u^*\hat{x})\bar{T}'] + u^*.\hat{z} = \nabla^2 T^* \quad (3.2)$$

$$\begin{aligned} \sigma_m\partial b^*/\partial t = \partial u^*/\partial x + \nabla^2 b^* \\ \sigma_m R[\bar{b}\partial u^*/\partial z - \bar{b}'(u^*.\hat{x})\hat{z} + (b^*.\hat{x})\bar{w}'\hat{z} - \bar{w}\partial b^*/\partial z] \end{aligned} \quad (3.3)$$

$$(\partial/\partial t + R\bar{w}\partial/\partial z)C^* = 0 \quad (3.4)$$

$$\nabla u^* = 0, \quad \nabla b^* = 0 \quad (3.5)$$

Here the accent denotes differentiation of the basic state variables with respect to the argument  $x$ . Note that the perturbation equations are linearised by neglecting all products of perturbation variables.

Our purpose here is to examine the stability of the basic state to the disturbance of the interface at  $x = 0$ . We then assume that the interface is disturbed infinitesimally by

$$\varepsilon\eta(y,z,t) = \varepsilon \exp[i(my+nz) + \Omega t] + c.c \quad (3.6)$$

The perturbation variables then take the form

$$\{u^*, p^*, T^*\} = \{iu, v, w, iup, T\} \eta(y,z,t) \quad (3.7)$$

where the variables in the curly brackets on the right of (3.7) are functions of  $x$  only.

Let us examine the simplest case in which there is no rotation, i.e., when  $\Omega = 0$ .

#### Non-rotating single line interface

We first write the equations in component form

$$(D^2 - a^2 - \Omega_*)u = nDp \quad (3.8)$$

$$(D^2 - a^2 - \Omega_*)v = -mnDp \quad (3.9)$$

$$(D^2 - a^2 - \Omega_*)w - iR\bar{w}'u + C + T = -n^2p \quad (3.10)$$

$$(D^2 - a^2 - \sigma\Omega_*)T - i\sigma R\bar{T}'u - w = 0 \quad (3.11)$$

$$Du + mv + nw = 0 \quad (3.12)$$

$$\Omega C = 0 \quad (3.13)$$

where  $a$  and the Doppler-shifted frequency are defined by

$$\Omega_* = \Omega + inR\bar{w}(x), \quad a^2 = m^2 + n^2 \quad (3.14)$$

It follows from (3.13) and (3.14) that  $C=0$ .

The equations (3.8) - (3.12) must be solved subject to the condition that all perturbation variables decay to zero as  $x \rightarrow \pm\infty$  ( or satisfy the appropriate radiation conditions ). Also the variables and their derivatives must satisfy certain compatibility conditions across the interface described by (3.6). These conditions arise from the requirement that the interface be a material surface and that the full variables and the

fluxes of momentum and heat be continuous across the interface. Using (3.12) and continuity of velocity, it may be shown that continuity of momentum flux normal to the interface reduces simply to continuity of pressure. Since the basic state vertical velocity has a discontinuous second derivative at  $x = 0$ , the perturbation vertical velocity must have an offsetting discontinuity in its first derivative. The full set of conditions can be summarized as follows:

- (i)  $u, v, w, p$  and  $T$  decay to zero as  $|x|$  increases indefinitely
- (ii)  $u, v, w, p, T, Dv$  and  $DT$  are continuous at  $x = 0$
- (iii)  $Dw(x_0^-) - Dw(x_0^+) = 1$
- (iv)  $R u = -i \Omega^* \quad \text{at} \quad x = 0 \quad (3.15)$

We note that equations (3.8) - (3.10) and (3.12) give

$$(D^2 - a^2)p - T + 2iR\bar{w}'u = 0 \quad (3.16)$$

and (3.10), (3.11) and (3.16) govern the evolution modes so that only three modes are present.

In order to ascertain that the instabilities identified below are due solely to the presence of material composition let us examine the case when there is no interface. Here we must revert to dimensional quantities since the non-dimensionalization used the amplitude of the concentration of the light material  $C$ . We can assume that the  $x$ -dependence is  $\exp(ix)$  since the equations have constant coefficients in this particular case. The dispersion relation is

$$(vh^2 + \Omega) \left[ (vh^2 + \Omega)(\kappa h^2 + \Omega)h^2 + \alpha\gamma g(r^2 + m^2) \right] = 0 \quad (3.17)$$

in which  $h^2 = r^2 + a^2$ . The solutions are

$$\Omega = vh^2, \quad -\frac{1}{2}h^2(v + \kappa) \pm \frac{1}{2} \left[ h^4(v - \kappa)^2 - 4\kappa\alpha\gamma g \frac{(r^2 + m^2)}{h^2} \right]^{1/2} \quad (3.18)$$

This readily shows that all three modes decay to zero.

When  $R$  is non-zero, we shall assume that  $R$  is small and adopt an expansion in the small parameter  $R$ . Thus

$$\{u, v, w, p, T\} = \sum_{s=0}^{\infty} \{u_s, v_s, w_s, p_s, T_s\} R^s, \quad \Omega = \sum_{s=1}^{\infty} \Omega_s R^s \quad (3.19)$$

We substitute (3.19) into (3.9) - (3.12), (3.16) and (3.15), and equate the coefficients of the various powers of  $R$  to zero to obtain a hierarchy of systems of equations which can be solved in succession. We need only consider the first two such systems in order to close the stability problem to leading order.

#### Problem 0

The leading order terms give

$$\begin{aligned} (D^2 - a^2)p_0 - T_0 &= 0 \\ (D^2 - a^2)w_0 + T_0 + n^2 p_0 &= 0 \\ (D^2 - a^2)T_0 - w_0 &= 0 \\ (D^2 - a^2)v_0 = -mnp_0 \quad Du_0 + mv_0 + nw_0 &= 0 \end{aligned} \quad (3.20)$$

These equations allow solutions of the form  $\exp(\lambda x)$  so that (3.20) gives

$$\begin{aligned} \mu p_0 - T_0 = \mu w_0 + T_0 + n^2 p_0 = \mu T_0 - w_0 &= 0 \\ \mu v_0 + m n p_0 = \lambda \operatorname{sgn}(x) u_0 + m v_0 + n w_0 &= 0 \end{aligned} \quad (3.21)$$

where

$$\mu = \lambda^2 - a^2 \quad (3.22)$$

Straightforward application of the boundary conditions (i) yields the solution



$$\{u_0, v_0, w_0, p_0, T_0\} = \sum_{j=1}^3 \{-n\lambda_j \operatorname{sgn}(x), -mn, \mu_j^3, \mu_j, \mu_j^2\} A_j \exp(-\lambda_j |x|) \quad (3.23)$$

The boundary remaining conditions give

$$\sum_{j=1}^3 \lambda_j A_j = 0, \quad \sum_{j=1}^3 \mu_j^3 \lambda_j A_j = \frac{1}{2}, \quad \sum_{j=1}^3 \mu_j^2 \lambda_j A_j = 0 \quad (3.24)$$

$$A_j = \frac{\mu_j^2}{2\lambda_j(3n^2 + 2\mu_j)}, \quad (3.25)$$

$\lambda_j$  are given by

$$\mu_j^3 + \mu_j + n^2 = 0 \quad (3.26)$$

and (3.22), provided we impose the condition that  $\operatorname{Re}(\lambda_j) > 0$ . We also find that

$$\Omega_1 = 0 \quad (3.27)$$

The leading order solution represents a neutral standing wave so that it merely undulates the interface in conformity with the basic state.

#### Problem 1

Here the equations take the form

$$\begin{aligned} (D^2 - a^2)p_1 - T_1 &= F_p \\ (D^2 - a^2)w_1 + T_1 + n^2 p_1 &= F_w \\ (D^2 - a^2)T_1 - w_1 &= F_T \\ (D^2 - a^2)v_1 &= -mnp_1 + in\bar{w}v_0 \\ Du &= mv - nw \end{aligned} \quad (3.28)$$

where

$$F_p = -2i\bar{w}'u_0, \quad F_w = in\bar{w}w_0 + i\bar{w}'u_0, \quad F_T = i\sigma[n\bar{w}T_0 + \bar{T}'u_0] \quad (3.29)$$

The solution of (3.28) and (3.29) can be obtained in the form of complementary function and particular integral :

$$y_1 = y_c = y_p \quad (3.30)$$

Using the superscripts + and - to refer to solutions in the regions  $x > 0$  and  $x < 0$ , respectively, we have

$$\{w_c^\pm, p_c^\pm, T_c^\pm\} = \pm \sum_{j=1}^3 \{\mu_j^3, \mu_j, \mu_j^2\} iB_j \exp(-\lambda_j |x|) \quad (3.31)$$

for the complementary function. The basic state solution for this case can be written in the form

$$\bar{w}^\pm = \pm \frac{1}{2} \operatorname{Im}[\exp(-k|x|)], \quad \bar{T}^\pm = \pm \frac{1}{2} \operatorname{Im}[i - i \exp(-k|x|)] \quad (3.32)$$

It then follows that

$$\{w_p^\pm, p_p^\pm, T_p^\pm\} = \pm \frac{1}{2} in \operatorname{Im} \left[ \sum_{j=1}^3 A_j \{w_j, p_j, T_j\} \exp[-(\lambda_j + k)|x|] \right] \quad (3.33)$$

in which

$$\begin{aligned} w_j &= D_j^{-1} [n^2 \gamma_j 2k\lambda_j + \gamma_j^2 (\mu_j^3 + k\lambda_j) - (\gamma_j + n^2) \sigma (\mu_j^2 - ik\lambda_j)] \\ p_j &= D_j^{-1} [-(1 + \gamma_j^2) 2k\lambda_j + \mu_j^3 + k\lambda_j + \sigma \gamma_j (\mu_j^2 - ik\lambda_j)] \\ T_j &= D_j^{-1} [n^2 2k\lambda_j + \gamma_j (\mu_j^3 + k\lambda_j) + \sigma \gamma_j^2 (\mu_j^2 - ik\lambda_j)] \\ D_j &= \gamma_j^3 + \gamma_j + n^2, \quad \gamma_j = (\lambda_j + k)^2 - a^2, \quad k = (1+i)/\sqrt{2} \end{aligned} \quad (3.34)$$

We can now use the last two in (3.28) to find that

$$v_{\pm}^{\dagger} = \pm iaB_4 \exp(-akl) \mp imn \sum_{j=1}^3 B_j \exp(-\lambda_j kl) \\ \pm \frac{1}{2} in \operatorname{Im} \left\{ \sum_{j=1}^3 A_j v_j \exp[-(\alpha_j + k)kl] \right\} \quad (3.35)$$

$$u_{\pm}^{\dagger} = \pm imB_4 \exp(-akl) - in \sum_{j=1}^3 B_j \lambda_j \exp(-\lambda_j kl) \\ + \frac{1}{2} in \operatorname{Im} \left\{ \sum_{j=1}^3 A_j u_j \exp[-(\alpha_j + k)kl] \right\} \quad (3.36)$$

where

$$v_j = -mn \frac{(p_j + 1)}{\gamma_j}, \quad u_j = \frac{(mv_j + nw_j)}{\lambda_j + k} \quad (3.37)$$

Application of the boundary conditions yield the relations

$$\sum_{j=1}^3 \{ \mu_j^3, \mu_j, \mu_j^2 \} B_j = \{ \hat{w}, \hat{p}, \hat{T} \} \quad (3.38)$$

$$aB_4 - mn \sum_{j=1}^3 B_j = \hat{v}, \quad \Omega_2 = -mB_4 + n \sum_{j=1}^3 \lambda_j B_j + \hat{u} \quad (3.39)(3.40)$$

in which

$$\hat{y} = -\frac{1}{2} n \operatorname{Im} \left[ \sum_{j=1}^3 A_j y_j \right] \quad (3.41)$$

It then follows that

$$B_j = -\frac{[\mu_j^2 \hat{T} + \mu_j \hat{w} - n^2 \hat{p}]}{\mu_j [3n^2 + 2\mu_j]}, \quad B_4 = \hat{v}/a - m(\hat{w} + \hat{p})/an \quad (3.42)$$

We can now use (3.40) to express the growth rate in the form

$$\Omega_2 = c_0 + \sigma c_1 \quad (3.43)$$

where

$$c_r = \hat{u}_r - \frac{m}{a} \hat{v}_r + \left[ \frac{m^2}{an} - nM_1 \right] \hat{w}_r + \left[ \frac{m^2}{an} + n^3 M_0 \right] \hat{p}_r - nM_2 \hat{T}_r \quad (3.44)$$

for  $r=0,1$  where

$$M_k = \sum_{j=1}^3 \frac{\lambda_j \mu_j^{k-1}}{(3n^2 + 2\mu_j)}, \quad \hat{y}_r = -\frac{1}{2} n \operatorname{Im} \left[ \sum_{j=1}^3 A_j y_{rj} \right], \\ y_j = y_{0j} + y_{1j} \quad (3.45)$$

When growth rate  $\Omega_2 > 0$ , the interface is unstable and its amplitude grows exponentially with time. The two terms in (3.43) can be taken to represent the influences of thermal diffusivity (i.e.,  $c_0$ ) and viscosity (i.e.,  $c_1$ ). The growth rate is computed as a function of the wavenumbers  $m$  and  $n$  for fixed values of the Prandtl number. The computations have shown that the interface is unstable for all values of the Prandtl number i.e., for any value of the Prandtl number, there is a pair of values  $(m, n)$  for which the growth rate is positive. Some of the results are illustrated in Figs. 8-11 below. We notice from Fig. 11 that the most unstable mode is three-dimensional for all Prandtl numbers greater than 0.065.

The growth rate varies as  $R^2$  and instability is present for all non-zero forcing (i.e., material concentration). The main cause of the instability can be traced down to the release of compositional energy and the horizontal temperature gradient.

### The rotating single line interface

Here we find it more convenient to scale the y-component of the velocity by

$$v \rightarrow nTa^{1/2}v \quad (3.46)$$

It is also found appropriate to define

$$\zeta = -i \operatorname{curl} u \quad (3.47)$$

and apply the operators  $\hat{z} \cdot \operatorname{curl}$ ,  $\hat{z} \cdot \operatorname{curl}^2$  to (3.1) and neglect magnetic effects to find the set of equations

$$w + \nabla^2 \zeta = F_1 \quad (3.48)$$

$$\nabla^4 w + n^2 Ta \zeta + \Delta i = F_2 \quad (3.49)$$

$$\nabla^2 p - T - Ta \zeta = F_4 \quad (3.50)$$

$$\nabla^2 T - w = F_3 \quad (3.51)$$

$$Dv = i\zeta - mu \quad (3.52)$$

$$Du = -Ta^{-1/2} mnv - nw \quad (3.53)$$

in which

$$F_1 = \Omega_* \zeta + nR\bar{w}v,$$

$$F_2 = \Omega_* \nabla^2 w + iR[n^2 \bar{w}'u + 2n\bar{w}'Dw + n^2 \bar{w}'w + \bar{w}'\Delta u + 2\bar{w}''Du + \bar{w}'''u],$$

$$F_3 = \Omega_* T + i\sigma RT'u$$

$$F_4 = -2iR\bar{w}'u$$

$$\Delta \equiv \nabla^2 - \partial^2 / \partial z^2 \quad (3.54)$$

The boundary conditions are

$$(i) \quad u, v, p, T, w, \zeta \rightarrow 0 \quad \text{as } |x| \rightarrow \infty$$

$$(ii) \quad u, v, p, T, w, DT, \zeta, D\zeta \quad \text{continuous at } x = 0$$

$$(iii) \quad Dw(0_-) - Dw(0_+) = 1$$

$$(iv) \quad i\Omega_* = R u(0) \quad (3.55)$$

The method of solution proceeds in the same way as in the case of the non-rotating interface. The leading order problem demands that  $m=0$  so that rotation inhibits three-dimensional motions. The solution is

$$\{w_0, T_0, \zeta_0, p_0\} = \pm \frac{1}{2} \sum_{n=1}^3 A_j \{\mu_j^3, \mu_j^2, -\mu_j^2, \mu_j(1-Ta)\} e^{\mp \lambda_j x}, \quad (3.56)$$

$$\{u_0^+, v_0^+\} = \pm \frac{1}{2} \sum_{n=1}^3 A_j \mu_j^2 \lambda_j^{-1} \{n\mu_j, i\} e^{\mp \lambda_j x} \quad (3.57)$$

in which

$$\zeta = \hat{z} \cdot \zeta \quad (3.58)$$

The next order problem provides an expression for the growth rate

$$\Omega_2 = \frac{n}{2} \left[ \bar{u} - M_2 \bar{w} + n^2 M_1 \bar{p} - (M_3 + \frac{Ta}{4} M_1) \bar{T} + \frac{Ta}{4} M_1 \bar{\zeta} \right] \quad (3.59)$$

Here

$$\zeta_j = -[w_j + \mu_j^2(\lambda_j + k) / \lambda_j] \quad (3.60)$$

The growth rate is examined as a function of the wavenumber  $n$  for fixed values of the Prandtl number. The main purpose here is to identify the influence of rotation on the stability of the interface. This is illustrated in Fig. 12.

Multiply (3.8) by  $u^{\#}$ , (3.9) by  $v^{\#}$  and (3.10) by  $w^{\#}$ , where the superscript # denotes the complex conjugate, and integrate to find

$$\operatorname{Re}(\Omega)E_M = -D_M + R \operatorname{re}(M) + \operatorname{Re}(B+J) \quad (3.61)$$

$$\operatorname{Im}(\Omega)E_M = -nRE_{WU} + R \operatorname{Im}(M) + \operatorname{Im}(B+J) \quad (3.62)$$

where

$$E_M = \int_{-\infty}^{\infty} |u|^2 dx, \quad D_M = \int_{-\infty}^{\infty} \left[ \left| \frac{du}{dx} \right|^2 + a^2 |u|^2 \right] dx,$$

$$M = -i \int_{-\infty}^{\infty} \frac{d\bar{w}}{dx} u w^{\#} dx, \quad E_{WU} = \int_{-\infty}^{\infty} \bar{w} |u|^2 dx \quad (3.63)$$

$$J = w^{\#}(0) \left[ \frac{dw}{dx}(0-) - \frac{dw}{dx}(0+) \right], \quad B = \int_{-\infty}^{\infty} w^{\#} T dx$$

Next we multiply the complex conjugate of (3.11) by  $T$  and integrate to get

$$\sigma \operatorname{Re}(\Omega)E_T = -D_T + \sigma R \operatorname{Re}(H) - \operatorname{Re}(B), \quad (3.64)$$

$$-\sigma \operatorname{Im}(\Omega)E_T = n\sigma R E_{WT} + \sigma R \operatorname{Im}(H) - \operatorname{Im}(B) \quad (3.65)$$

in which

$$E_T = \int_{-\infty}^{\infty} |T|^2 dx, \quad D_T = \int_{-\infty}^{\infty} \left[ \left| \frac{dT}{dx} \right|^2 + a^2 |T|^2 \right] dx$$

$$H = i \int_{-\infty}^{\infty} \frac{d\bar{T}}{dx} u^{\#} T dx, \quad E_{WT} = \int_{-\infty}^{\infty} \bar{w} |T|^2 dx \quad (3.66)$$

Note that the first terms in (3.61) and (3.62) represent the rate of change of wave kinetic energy,  $D_M$  represents the rate of viscous dissipation,  $M$  the rate of transfer of kinetic energy from the mean flow through the velocity shear, and  $B$  and  $J$  the rates of gain of wave energy by the action of buoyancy.  $B$  represents the

action of thermal buoyancy while  $J$  represents the action of compositional buoyancy resulting from the deformation of the interface.  $E_T$  represents the gain of wave potential energy,  $D_T$  the rate of thermal dissipation and  $H$  the rate transfer of energy from the basic state thermal profile to the perturbations.

Equations (3.61), (3.62), (3.64) and (3.65) give

$$\operatorname{Re}(\Omega)[E_M + E_T] = -(D_M + D_T) + R \operatorname{Re}(M + \sigma H) + \operatorname{Re}(J) \quad (3.67)$$

$$\operatorname{Im}(\Omega)[E_M - \sigma E_T] = nR(E_{WT} - E_{UV}) + R \operatorname{Im}(M + \sigma H) + \operatorname{Im}(J) \quad (3.68)$$

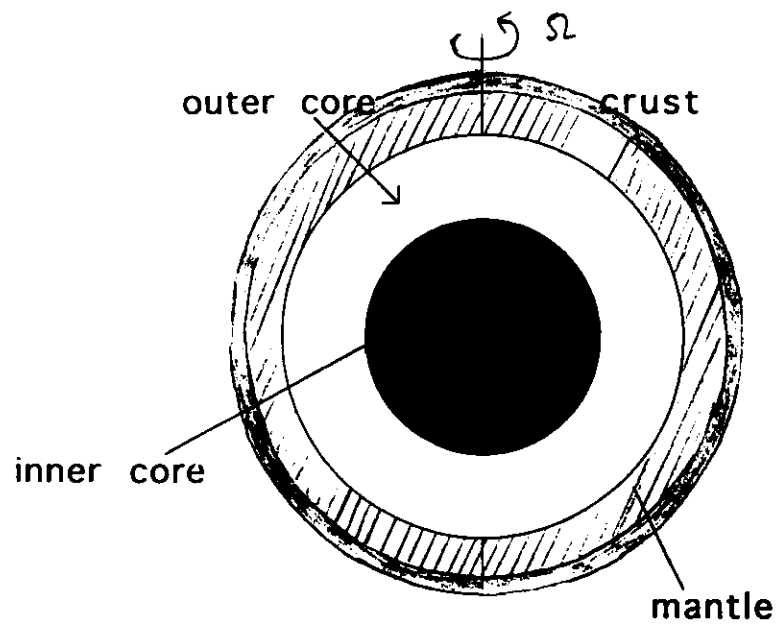
These last two equations show the strong influence of the jump in material concentration on the growth rate and frequency of the disturbance. The solutions obtained above yield

$$0 = -(D_{M0} + D_{T0}) + w_0^{\#} \quad (3.69)$$

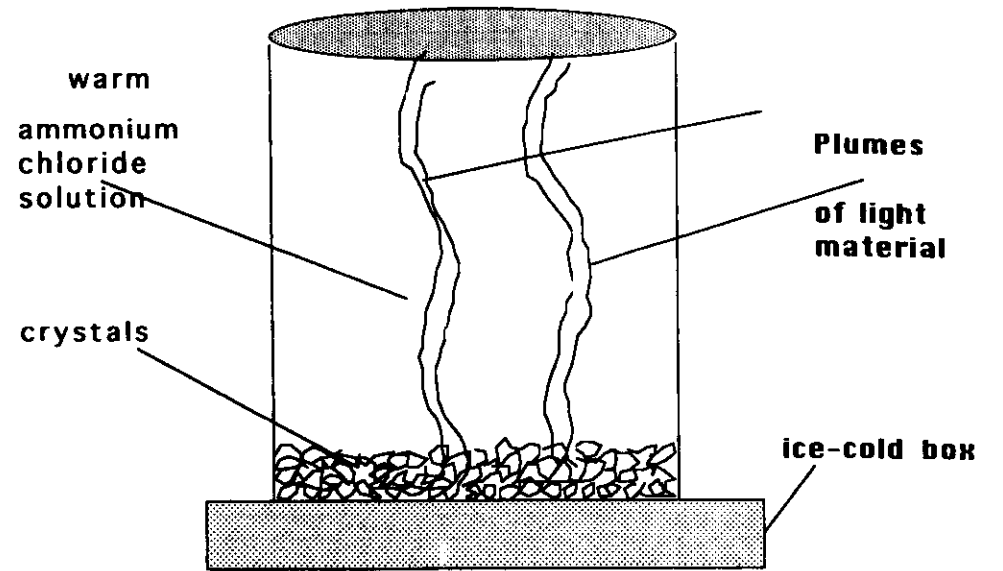
so that the major part of the dissipation is counterbalanced by the release of compositional energy. Higher orders show the contribution of transfer of energy from the basic state to the wave to enhance instability.

## REFERENCES

- CHANDRASEKHAR,S.1961 *Hydrodynamic and hydromagnetic stability*. Oxford, Clarendon Press .
- DUDIS,J.J. & DAVIS,S.H. 1971 ' Energy stability of the buoyancy boundary layer '. *J.Fluid Mech.* **47** , 381-403.
- ELTAYEB,I.A. 1972 ' Hydromagnetic convection in a rapidly rotating fluid layer '. *Proc. Roy. Soc. Lond.* **A326** , 229-254.
- ELTAYEB,I.A. 1975 ' Overstable hydromagnetic convection in a rotating fluid layer '. *J.Fluid Mech.* , **71** , 161-179.
- ELTAYEB,I.A. 1981 ' Propagation and stability of wave motions in rotating magnetic systems ' . *Phys. Earth Planet.Interiors* **24** , 259-271.
- ELTAYEB , I.A. 1992.'The propagation and stability of linear wave motions in rapidly rotating spherical shells : Weak magnetic fields '. *Geophys. Astrophys. Fluid Dyn.* **67** , 211-239.
- ELTAYEB,I.A. & KUMAR,S. 1977 ' Hydromagnetic convective instability of a rotating , self-gravitating fluid sphere containing a uniform distribution of heat sources'. *Proc. Roy. Soc.Lond.* **A 353** , 145-162
- ELTAYEB,I.A. & LOPER,D.E. 1991 ' On the stability of vertical double-diffusive interfaces. Part 1 . A single line interface '. *J.Fluid Mech.* **228** , 149-181.
- ELTAYEB,I.A. & LOPER,D.E. 1994 ' On the stability of vertical double-diffusive interfaces. Part 2 . Two parallel interfaces '. *J.Fluid Mech.* (to appear).
- FEARN , D.R. 1979. ' Thermally driven hydromagnetic convection in a rapidly rotating sphere '. *Proc.Roy.Soc.Lond.* **A 369** , 227-242.
- GILL,A.E. & DAVEY,A. 1969 ' Instabilities of a buoyancy -driven system' *J.Fluid Mech.* **35** , 775-798.
- LOPER,D.E. 1983 'Structure of the inner core boundary '. *Geophys.Astrophys.Fluid Dyn.* **25** , 139-155.
- LOPER,D.E. 1984 'Structure of the core and lower mantle '.*Advances Geophys.* **26** , 1-34.
- LOPER,D.E. & ROBERTS,P H. 1983 'Compositional Convection and the gravitationally powered dynamo '. *In " Stellar and planetary magnetism "* ( A.M.Soward,ed.) , pp.297-327. Gordon & Breach , New York.
- MOFFATT,H.K. 1978 . *Magnetic field generation in electrically conducting fluids*. Cambridge University Press.
- ROBERTS,P.H. & LOPER,D.E. 1983 . 'Towards a theory of the structure and evolution of a dendrite layer '. *In " Stellar and Planetary Magnetism "* ( A.M.Soward, ed.) , pp. 329-349. Gordon & Breach,New York



THE EARTH AND ITS DIVISIONS



THE AMMONIUM CHLORIDE EXPERIMENT

*Figure 10*

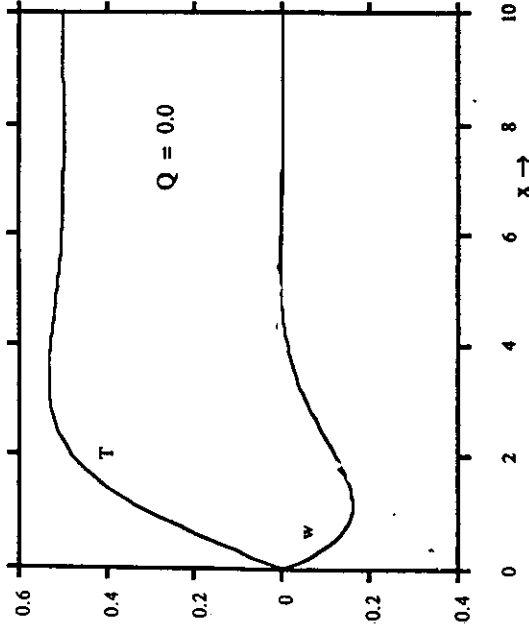
zed  
lled a  
on  
ace  
y is  
and  
ite  
the  
s to  
the  
ous,  
nce  
of a  
two  
ity  
ibly  
re a  
a to  
dge  
the  
able  
tem  
lity  
of  
shan  
&  
ome  
ll &  
rent  
wall  
must  
sires  
e of  
wall  
nore  
tion  
ly is  
elow  
onal  
t the  
both  
; the



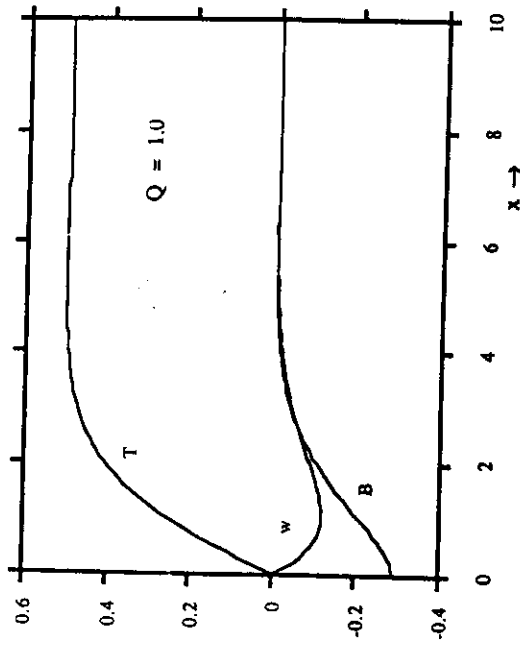
FIGURE 1. Plumes of fresh water emanate from chimneys which form spontaneously within a porous matrix of  $\text{NH}_4\text{Cl}$  crystals when a warm aqueous solution of ammonium chloride and water is cooled from below. The compositionally buoyant plumes exhibit a helical instability.

Figure 2b

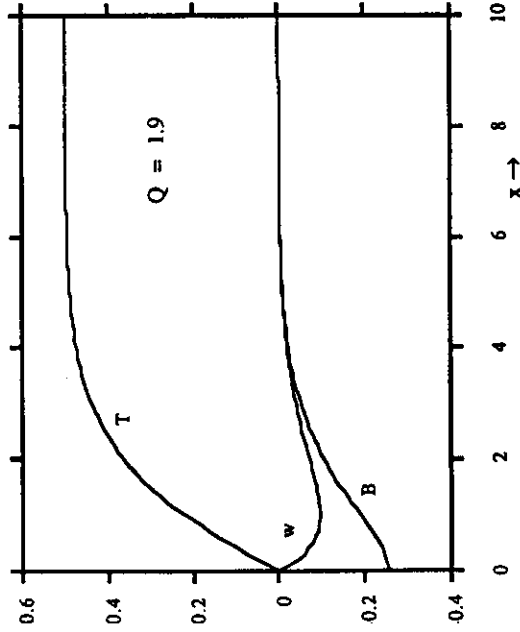
Single Line Plume Basic Solutions



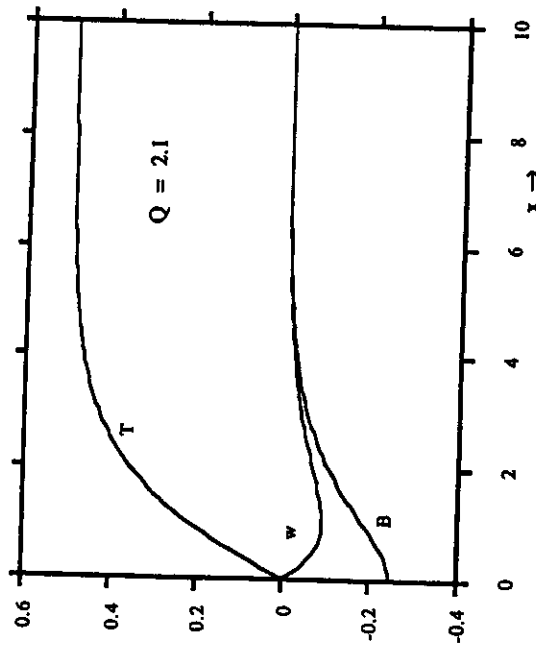
Single Line Plume Basic Solutions



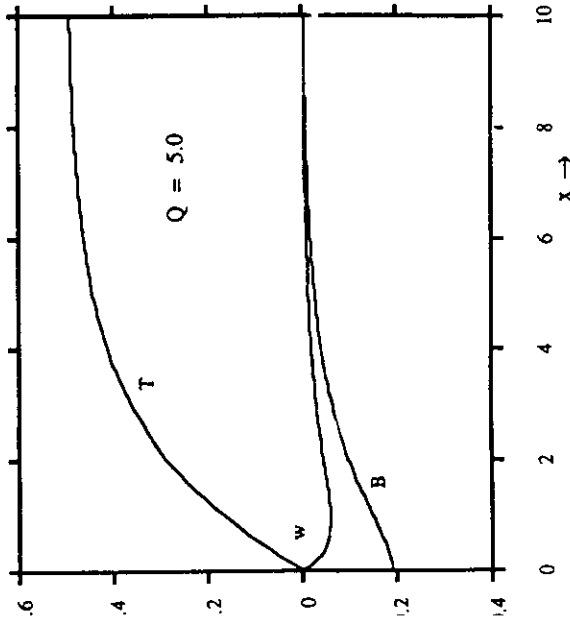
Single Line Plume Basic Solutions



Single Line Plume Basic Solutions



Single Line Plume Basic Solutions



Note that the magnetic field suppresses the oscillations.

Figure 3



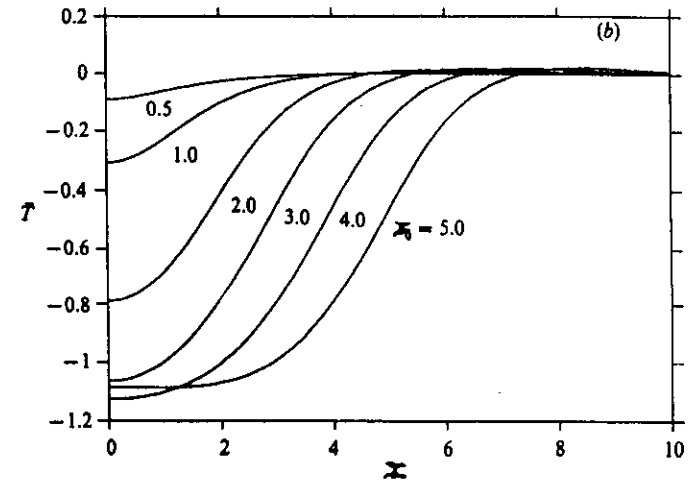
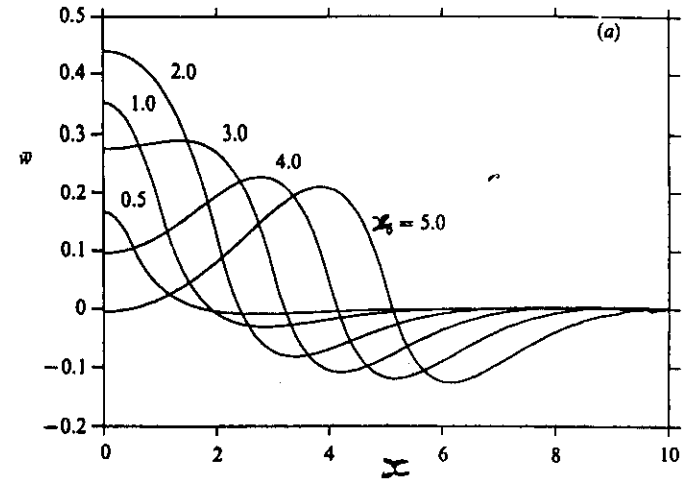
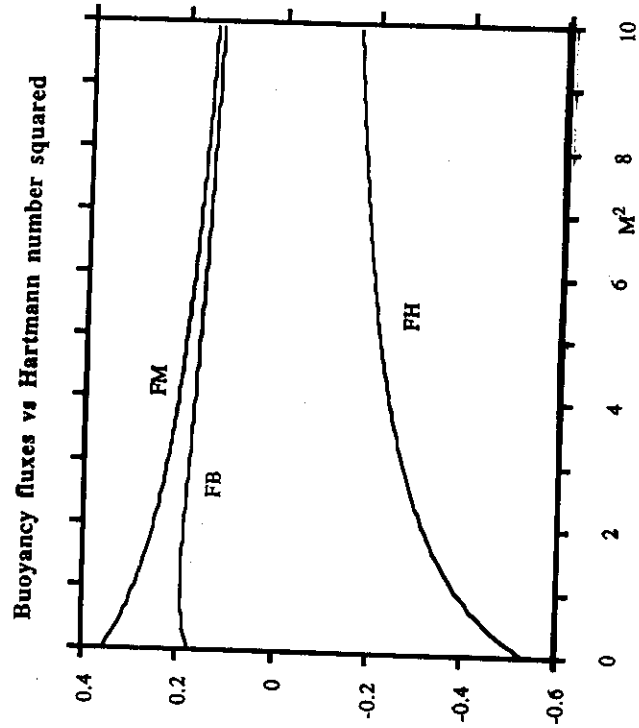


FIGURE 5. (a) The basic-state vertical velocity,  $w$ , and (b) temperature,  $T$ , plotted versus  $x$  for values 0.5, 1.0, 2.0, 3.0, 4.0 and 5.0 of  $x_0$ .

Figure 4.

Figure 5a, b

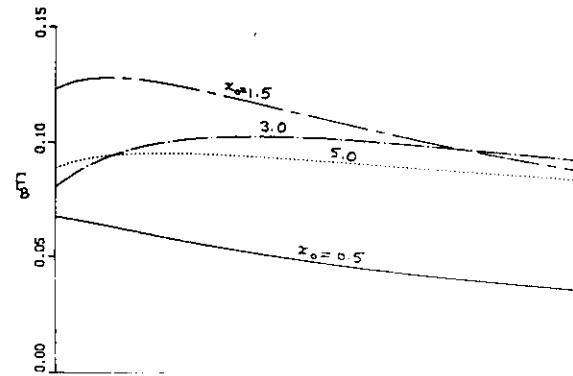
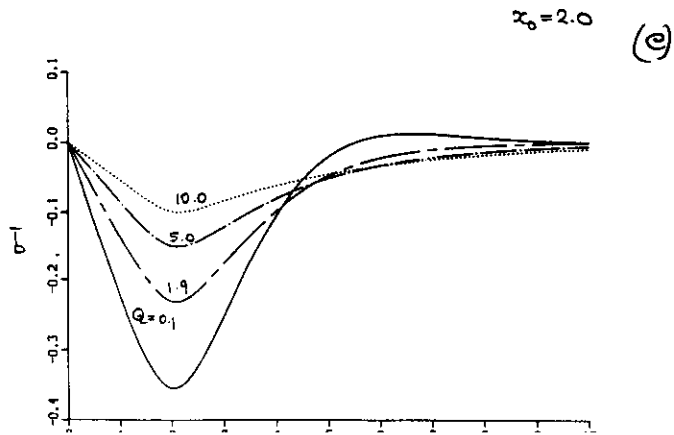
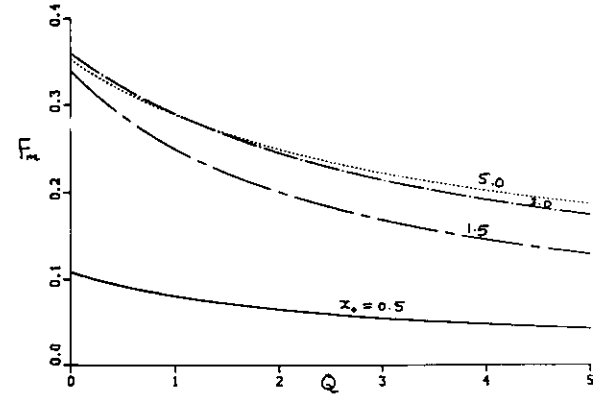
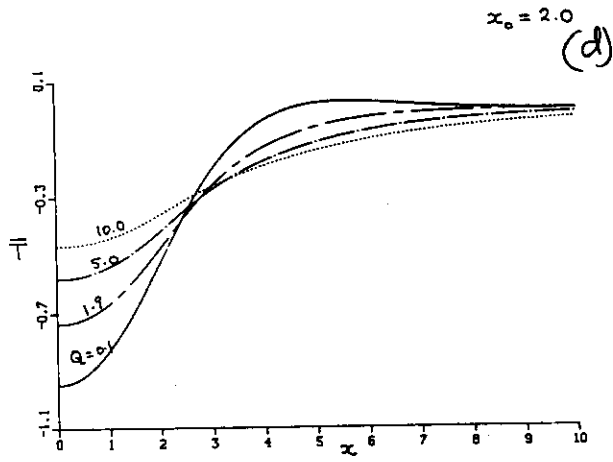
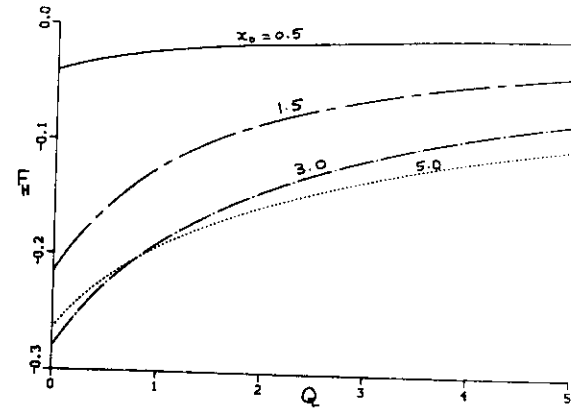
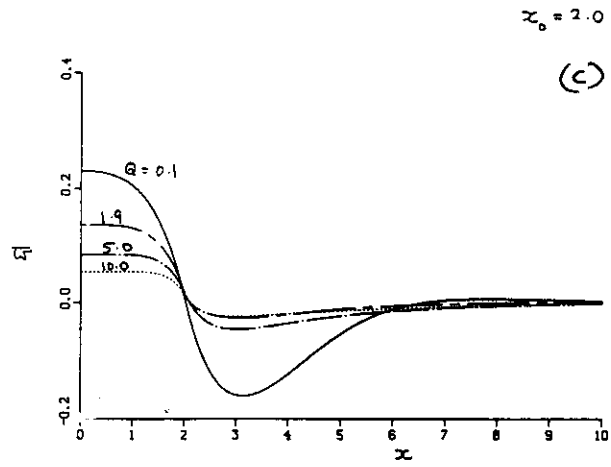
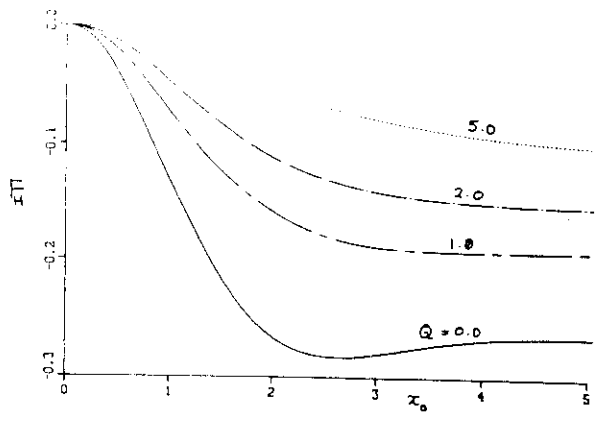
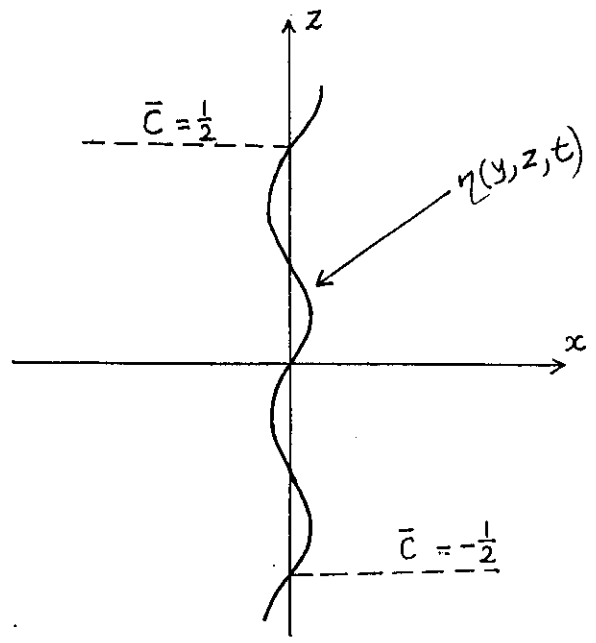


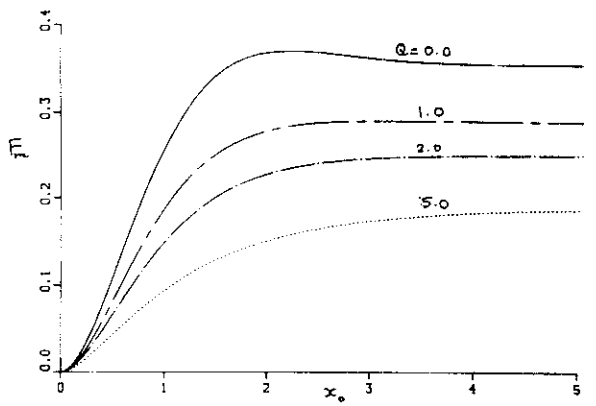
Figure 5 side

~~Figure 6a~~

The single Line plume



vs  $x_0$



$$\Omega_2 = F_1^{(0)}(n, Ta) + \sigma F_2^0(n, Ta)$$

Figure 7

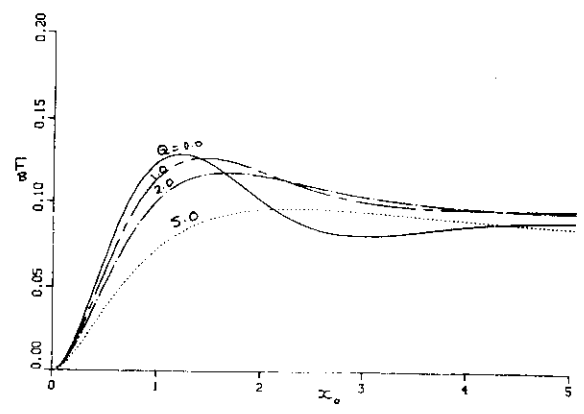


Figure 6b

Stability of vertical double-diffusive interfaces. Part 1

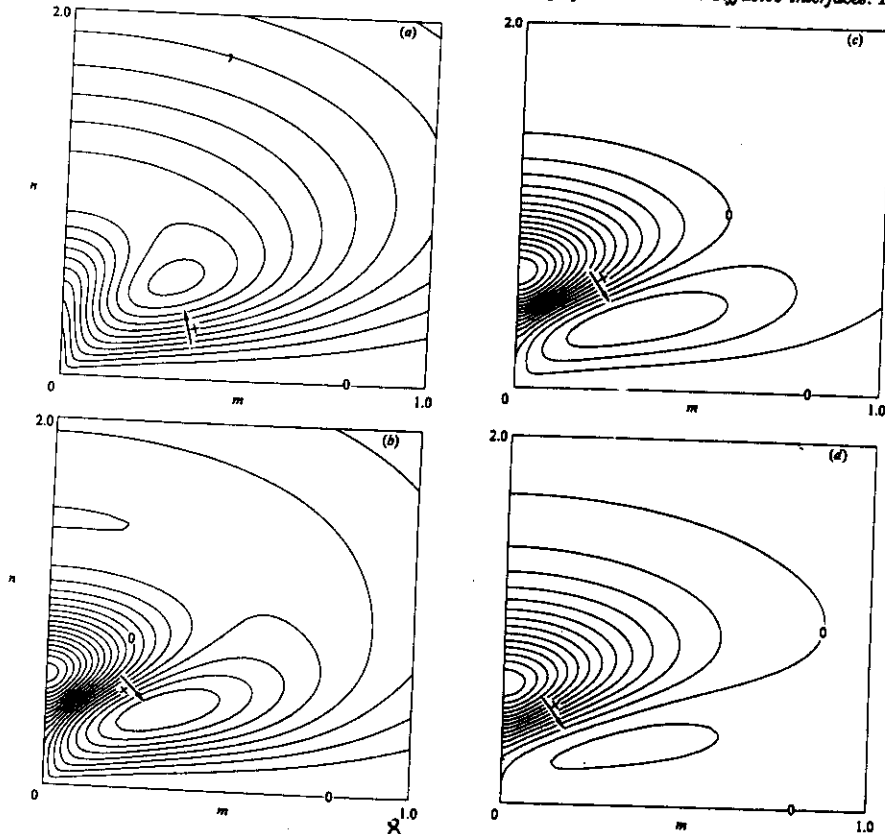


FIGURE 8. Isolines of the growth rate,  $\Omega_1$ , for the single plane interface for four representative values of the Prandtl number  $\sigma$ : (a)  $\sigma = 1.0$  (minimum value 0, maximum value 0.00570, contour interval 0.0005); (b)  $\sigma = 3.0$  (minimum value  $-0.00580$ , maximum value 0.00448, contour interval 0.0005); (c)  $\sigma = 5.0$  (minimum value  $-0.0139$ , maximum value 0.00394, contour interval 0.001); (d)  $\sigma = 10.0$  (minimum value  $-0.0345$ , maximum value 0.00336, contour interval 0.0025).

Figure 8

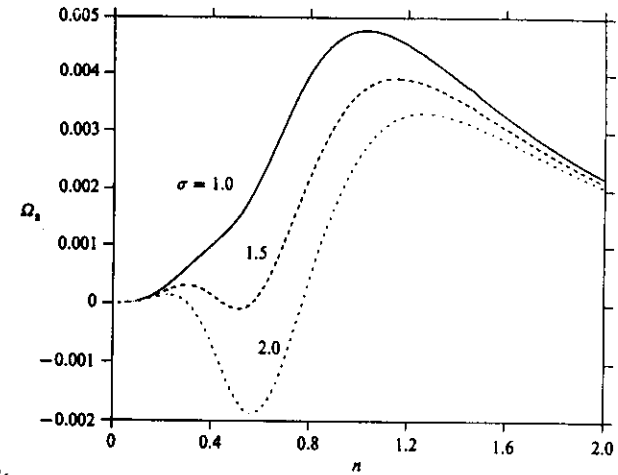


FIGURE 9. The profile of the growth rate  $\Omega_1$  of the single plane interface when the horizontal wavenumber  $m = 0$  for three different values of the Prandtl number  $\sigma$  near  $\sigma = \sigma_c \approx 1.472$ , to illustrate the manner in which the region of instability develops with increasing  $\sigma$  for moderate values of the vertical wavenumber  $n$ .

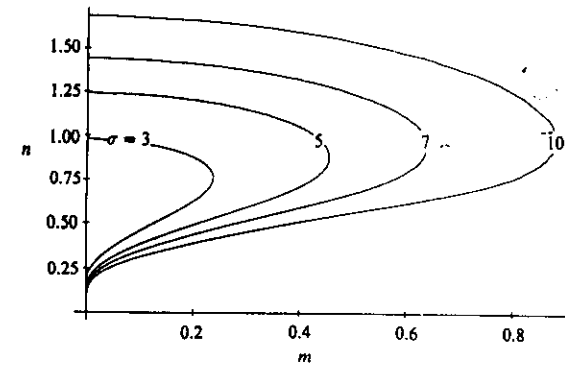


FIGURE 10. The regions of stability for the single plane interface in the  $(m, n)$  wavenumber plane for various values of the Prandtl number  $\sigma$ , as labelled. The region of stability lies within the respective curve and instability prevails outside. No stability is possible if  $\sigma < 1.472$ .

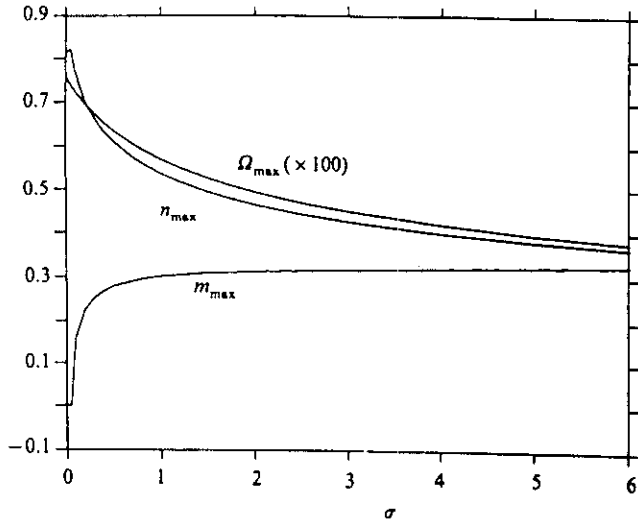


FIGURE 11. The maximum growth rate  $\Omega_{\max}$  and the associated wavenumbers  $m_{\max}$  and  $n_{\max}$  for the single plane interface as a function of the Prandtl number  $\sigma$ . Note that  $m_{\max} = 0$  for  $\sigma \leq 0.065$ .

The maximum growth rate for the rotating single line interface as a function of the Taylor number for various values of  $\sigma$ , as labelled.

